Biophysical Chemistry 143 (2009) 44–54

Contents lists available at ScienceDirect

Biophysical Chemistry

journal homepage: http://www.elsevier.com/locate/biophyschem

Mathematical model of a network of interaction between p53 and Bcl-2 during genotoxic-induced apoptosis

Yasam Dogu, José Díaz *

Theoretical and Computational Biology Group, Facultad de Ciencias, Universidad Autónoma del Estado de Morelos, Av. Universidad 1001, Colonia Chamilpa, Cuernavaca, Morelos, México 62209

ARTICLE INFO

Article history:
Received 27 December 2008
Received in revised form 25 March 2009
Accepted 25 March 2009
Available online 5 April 2009

Keywords:
p53
Genotoxic damage
Apoptosis
Modular network
Nonlinear dynamics
Puma

ABSTRACT

Ionizing radiation like UV light, gamma and X rays, can produce genotoxic damage in fibroblast cells. This injury can be reverted by activation of specific nuclear molecules. However, intense genotoxic damage induces the activation of the p53 dependent apoptotic pathway. Activated nuclear p53 has the role of a transcription factor that switches on the transcription of the Puma protein, which once released into the cytoplasm leads to the activation of a network of chemical processes that produces cell death. This network is built up with the chemical interaction between pro-apoptotic p53, Puma and Bax proteins and the anti-apoptotic Bcl2 and Bcl-x_L proteins. In this work we present a mathematical model of this modular network under different regimes of Puma release into the cytoplasm. In this model we use a set of coupled nonlinear differential equations, which is solved by numerical methods, to determine the nature of the equilibrium points of the dynamical system. With this information we construct the phase portrait associated with Puma induced apoptosis and we found that once the genotoxic injury is produced, Bax levels continuously increase. In this work we propose that a possible mechanism for the control of apoptosis is the Bax level in the cytoplasm, i.e., Bax is continuously released into the cytoplasm, even in absence of Puma, according to the kinetic properties of the set of chemical interactions in which the Bcl2/Bax complex takes part. If the damage is reverted before the Bax level reaches a threshold value the apoptotic process is stopped, otherwise the process goes on until cell death.

1. Introduction

A cancer cell can be considered as a pathological dynamical state of a complex system, i.e., of a normal cell. Cells can reach this illness state in various forms but generally this anomaly is due to a malfunction of a specific set of proteins that lose their role in cellular homeostasis [1], including apoptosis or programmed cellular death. Once the apoptosis mechanism is damaged, cells can proliferate without control [2]. In this case, changes in parameters of the dynamical system can induce a very resistant, and difficult to revert, pathological robust state.

Genes that participate in oncogenesis are the result of the transformation of the genes that normally control cell cycle, damaged-DNA repair and cellular adherence [1]. Cell transformation into a cancer one requires at least of two mutations: a) a mutation in a tumor suppressor gene and b) a mutation in a proto-oncogene that give rise to an oncogene [1]. When these DNA changes cannot be repaired, cell falls into the first steps of malignant transformation [1,2].

1.1. Molecular mechanisms of apoptosis

Apoptosis is a complex of molecular processes that is highly dependent on the cell type. In the case of thymocytes, DNA damage produces a fast induction of apoptosis. In contrast, in primary fibroblast the response to DNA damage is slower [4]. Norbury and Zhivotovsky point out that this dissimilarity could reflect a substantial difference in the expression of the relative content of pro- and anti-apoptotic molecules that set up a characteristic threshold for the response to DNA damage in each cellular type [4].

There are two ligand activated or extrinsic apoptotic pathways. The extrinsic pathway type I is activated by the binding of a FAS death ligand (FASL) to the FAS receptor (FASR) on the cell surface [5]. FAS is a member of the Tumour Necrosis Factor (TFN) gene super family, thus TFN can also activate this pathway when binding to its cell surface receptor (TFNR) [5,3]. The formation of the ligand-receptor complex in both cases induces the formation of a death-induced signalling complex (DISC) [6]. In the case of FAS, the DISC is built when a set of activated FASR form a cluster that allows the binding of the adapter FADD (FAS-associated death domain) protein [5,3]. This DISC allows two molecules of procaspase-8 move closer to one another to exercise mutual proteolytic cleavage and become activated caspases-8 [6]. DISC can also activate caspase-10, which is an initiator caspase like caspase-8 [6].

* Corresponding author. Tel.: +52 777 3297020; fax: +52 777 3297040.
E-mail address: biofisica@yahoo.com (J. Díaz).

0301-4622/$ – see front matter © 2009 Elsevier B.V. All rights reserved.
doi:10.1016/j.bpc.2009.03.012

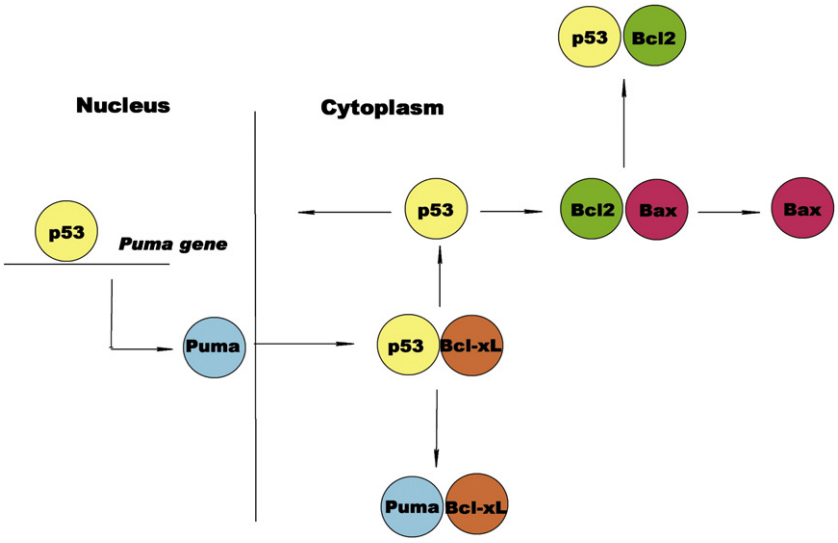

Fig. 1. Molecular interactions in the cytoplasm of a cell under an apoptotic stimulus. Puma is released to the cytoplasm and produces a chain of reactions that finally leads to the formation of the Bax/Bax homodimer in the outer membrane of mitochondria.

Activated caspases 8 and 10 have caspases 3, 6 and 7 as proteolytic cleavage targets. The last conform a group of effectors caspases [3]. Once these caspases are activated cell suicide becomes irreversible [6].

The extrinsic apoptotic pathway type II shows low levels of activated caspase-8. The amplification of the death signal is due to the proteolytic cleavage of Bid by caspase-8, leading to a truncated form of Bid o tBid, which is translocated into the neighbourhood of the mitochondria's membrane where it acts through the Bcl2-mediated activation of Bax to induce the release of cytochrome c into the cytoplasm. The result is the activation of caspase-9 and of the effector caspase 3 [3,5,6].

Stress, UV-light or chemo toxic substances usually activate the intrinsic apoptotic pathway. This pathway is controlled by the activation of the ATM/ATR set of kinases that senses single and double DNA strand damage [3,6,7]. ATM phosphorylates the nuclear protein p53 on serine 15. The DNA damage also induces the phosphorylation of p53 on serine 20 by Chk1 and Chk2 kinases. These chemical changes in p53 avoid its ubiquitination by the ubiquitin E3 ligase Mdm2, which is also phosphorylated by ATM on serine 395 [7]. The p53-Mdm2 nuclear equilibrium is then broken [8].

As a consequence, nuclear active p53 increases its concentration and acquires enhanced transcriptional functions activating pro-apoptotic genes like *Puma* and *Bax*. The activation of this set of genes contributes to the initiation of the caspase cascade and cellular death [1–3].

In fibroblast cells, a pool of cytoplasmic p53 is associated with the protein Bcl-x_L [9]. When Puma is released into the cytoplasm it cleaves the Bcl-x_L/p53 complex [9,10] and liberates p53. Part of the free p53 migrates into the nucleus but the rest breaks the Bcl2/Bax complex by associating with Bcl2 and releases the protein Bax [11] (Fig. 1).

Bax forms a homodimer complex in the outer membrane of mitochondria. It is believed that this dimeric complex forms the ionic pore that allows the release of the cytochrome c from the mitochondria, inducing the so-called mitochondrial-dependent apoptosis [6].

1.2. Dynamical properties of apoptosis

Cell is a complex network of chemical and electrical processes. Each network is characterized by a set of parameters that characterize its dynamical features that include the response to environmental and internal inputs. This response is crucial for its survival and is characteristic of each cell type [12].

The analysis of cell dynamics is not an easy effort. The interactions among the nodes of a biochemical network could form a very intricate set of kinetic equations whose representation by differential equations implies a long number of parameters that in most of the cases are unknown [13].

However, the representations of a network by a continuous model conveys the use of the tools of the nonlinear dynamics analysis that, combined with the numerical solution of the ODE's, offers a detail qualitative description (and in sometimes also quantitative), of the system's fixed points and trajectories among them in the corresponding phase space [12,13].

Stability analysis, together with bifurcation analysis and experimental data, can be used to find the interval of values of a set of parameters for which the system presents a particular dynamical behaviour of interest. From this knowledge, we can perform a series of *in silico* experiments to investigate the performance of the system under simulated experimental conditions to guide future experimental work and understand the response of the system to perturbations from the external and internal cell's environment [12,13].

This approach is useful in the case of the research on the dynamical aspects of apoptosis. Understanding from a dynamical point of view, in complement to the experimental approach, how the cell performs its own destruction (death o suicide) under normal conditions will help us to realize how in the pathological cell state the apoptotic process has been modified [5] and if these modifications can be reverted by means of pharmacological, genetic or other suitable therapeutic tools.

In this form, previous *in silico* experiments have explored the activation of the nuclear part of the intrinsic pathway under radiotherapy conditions [14]. Dose of the order of 15 Gy of ionizing radiation (IR) produces a high number of Double Strands Breakpoints (DSB's) in cancer cells to induce apoptosis [14]. The result of the application of this dose is the transition of ATM to its active state (ATM*) after 7 min reaching its steady state after 17 min. The subsequent activation of nuclear p53 by this kinase induces an oscillatory dynamics in the negative feedback loop p53-Mdm2. These oscillations have a period of about 400 min. However, the number and amplitude of these oscillations are IR dose-dependent and could be a p53-driven mechanism that ensures the elimination of the effects of the protein waste produced from DNA points that were incorrectly repaired [14]. In this form, this model predicts that the action of radiotherapy, from a dynamical point of view, conveys the existence of a molecular switch that sharply drives the system to a cycle in the p53-Mdm2 phase plane.

Other models coincides with the existence of this persistent cycle for the p53-Mdm2 loop for single cells, but also point out that in cell population an spiral attractor is observed instead [8,14,15].

The model proposed by Chickarmane et al. [8] consider the nuclear regulation loop of p53-Mdm2 but also takes into account the presence of the regulatory proteins Arf(p19), β-catenin, and Siah. The last one is an ubiquitin ligase that enhances the degradation of the constitutive protein β-catenin, which is a regulator of the *Arf* gene transcription. Arf protein sequesters Mdm2 from its substrates and promotes its degradation, enhancing the nuclear levels of phosphorylated p53. In this model the activation of the ATM kinase is also taken into account, but the bistable switch that turns "on" the p53-Mdm2 cycle is due to a positive feedback loop between ATM* and the Nbs-1* protein (* represents the active state of a molecule). This work characterize the qualitative dynamical behaviour of the ATM-driven p53-Mdm2 feedback loop and shows the existence of a limit cycle, which is reached through a supercritical Hopf bifurcation. This model also asserts, according to the results from a similar model [15], that the behaviour of the p53-Mdm2 loop is digital, i.e., the average amplitude and duration of the p53 and Mdm2 pulses are fixed, whereas their mean number increases with the strength of DNA damage.

Geva-Zatorsky et al. [16], in a theoretical-experimental work with a MCF7 cell line clone subject to different doses of gamma irradiation, found sustained oscillations of nuclear p53 and Mdm2 in single cells over a time interval of about ~36 h. The period of these oscillations was of the order of 5.5 h, and the fraction of cells that showed this periodic behavior after DNA damage increased with the IR dose. An interesting result from this work is that sustained oscillations can be transferred to daughter cells. However, they also found that the synchronization of the oscillations between cell populations is lost after a short period of time following the gamma irradiation and, consequently, oscillations appear to be damped after 2–3 peaks when analytical techniques like inmunoblots, which average over cell populations, are used.

Although the characteristics of the oscillations in single cells change from one type to other, is clear that in the nuclear compartment the activation of the dynamical characteristics of the DNA repairing molecular machinery conveys a trajectory that sharply leads to a unstable fixed point in the ATM*-p53-Mdm2 phase space, from which a limit cycle parallel to the p53-Mdm2 plane emerges through a supercritical Hopf bifurcation. However, there is also the possibility of the existence of a subcritical Hopf bifurcation, which can then lead to cycles of different IR-dose dependent amplitude [8,16].

In the case of the cytoplasmic compartment, previous work by Bagsi et al. [17] has studied the role of Bax and Bcl2 synthesis and degradation rates in mitochondria-dependent apoptosis, finding the existence of a saddle point bifurcation in the caspase 3-Bax degradation rate diagram. The Bax degradation rate of ~0.11 s^{-1} determines the upper limit to the region of bistability. Inside this region, the saddle point bifurcation can drive the system either to a stable point with a high concentration of caspase 3 (cell death) or to a stable point with a low concentration of caspase 3 (cell survival). Out of this region, the systems dynamics is settled on by the existence of a single stable fix point that determines cell surviving independently of the concentration of caspase 3.

One conclusion from this work is that a pathological state arises in cells when Bax degradation rate is above a threshold value, giving rise to a monostable cell survival dynamics, i.e., cells do not die. Otherwise cell death or survival occurs depending on the initial caspase-3 level [17–19].

Furthermore, Cui et al. work [18] points out that the activation of the "Bcl2 switch" upstream mitochondria induces apoptosis when the formation of the heterodimer Bak/Bax reaches a certain level. In both cases, Bax level settles on the beginning of the apoptosis process [17–19].

Fussenegger, Bailey and Varner work [5] used mass-conservation law and kinetic rate laws to establish a model of caspases 8 and 9 activation by the extrinsic and intrinsic apoptotic pathways respectively. According to their results, the fraction of activated caspase 8 has reach approximately 50% of its maximum value in less than ~10 min after the initiation of the apoptotic process by the binding of the death ligand to the FASR. Its maximum fraction of activation is reached after ~2 h. In contrast, the activation of caspase 9 starts ~20 min after the initiation of apoptosis. In this model, this time lag between the activation of the caspases 8 and 9 represents the time requiring for the release of cytochrome c from mitochondria.

In the case of the intrinsic pathway, the above model predicts that the release of cytochrome c begins ~10 min after the stress signal. The executioner caspases are active at 40% of its maximum value 1 h after the initiation of the stress response. 70% of them are active 2 h after. According to this model, a negative mutation in p53 decreases the fraction of both activated caspase 9 and executioner caspases.

According to the above antecedents, is clear that the role of pro-apoptotic proteins like p53 and Puma in the response to stress signals has not been taken into account in previous models. Therefore, in this work we set a mathematical model based on a series of differential equations that describes the temporal behavior of the p53-dependent interactions in the intrinsic apoptotic pathway (Fig. 1). This model predicts that: 1) the overall kinetic behavior of this net under a genotoxic stimulus is mainly due to a possible p53-induced release of Bax from its complex with Bcl2 even in absence of Puma; 2) the release of Puma in the cytoplasm increases the rate of liberation of Bax from the Bcl2/Bax complex.

From these model results, we propose that the possible mechanism of the control of apoptosis is the Bax level in the cytoplasm, i.e., once DNA damage is produced, Bax is continuously released into the cytoplasm from the Bcl2/Bax complex, even in absence of Puma, according to the kinetic properties of the set of chemical interactions in which this complex takes part (see Fig. 1). In consequence, if DNA damage is repaired cells may divide before Bax reaches a threshold value or may have a mechanism that controls Bax concentration prior to reach this threshold value [17,18]. In the network of p53 cytoplasmic dependent chemical interactions (Fig. 1) Puma plays the role of accelerator of the Bax level increasing process.

In order to test the certainty of the above proposal we perform a series of *in silico* experiments in which we vary the level of Puma in the cytoplasm to determine the cytoplasmic concentration of Bax in response to Puma's input. We use the network of p53-dependent cytoplasmic interactions of Fig. 1. In this network, the role of p53 is to enhance the level of free Bax in response to Puma's input. Although some authors have proposed the direct interactions of p53 with Bax, this interaction occurs in the nucleus [19–21], so we do not take into account this step in our model.

We think that this continuous release of Bax from its complex with Bcl2 is mainly due to the k_d (dissociation constant) value for this reaction, which is of the order of 0.01 μM [19]. This value indicates a relative weak binding of Bcl2 and Bax that makes easier the substitution of Bax by p53 in the complex (see Materials and methods section).

2. Materials and methods

2.1. Model description

2.1.1. Model cell

In this work, the human fibroblast cell is considered as a model, whose geometry is to be a large ellipsoid when the cell is not attached to a surface. This ellipsoid has mayor axes of ~20 μm and two equal minor axes of ~5 μm each. The nucleus is a sphere of ~5 μm of diameter. Thus, the effective cytoplasmic volume is ~196 μm^3 and the concentration of the molecules of the apoptotic pathway is referred to this volume.

2.1.2. Model description

In Fig. 2a we show the central role of Bcl-x_L in the subset of reactions that take place in the cytoplasm after intense DNA damage by ultraviolet or gamma rays [1]. In these reactions Puma substitutes

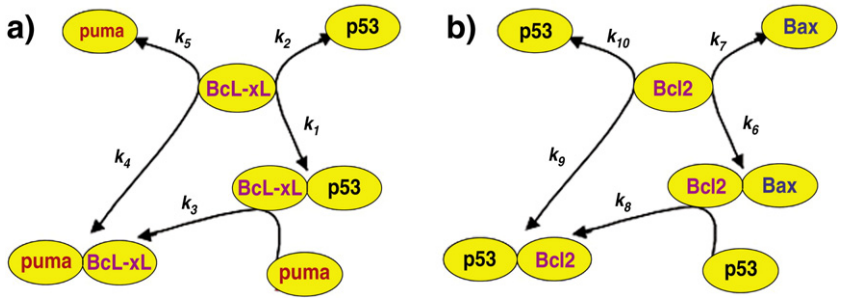

Fig. 2. a) Set of interactions between proteins Puma, Bcl-xL and p53. In this figure we show the central role of Bcl-x_L in these chemical reactions; b) Set of interactions between proteins p53, Bcl2 and Bax. The free cytoplasmatic p53 concentration is the key variable that leads this set of substitution chemical reactions until the final liberation of Bax from its complex with Bcl2. The value of the rate constants is shown in Table 3.

p53 in the Bcl-x_L/p53 complex and forms the new complex Bcl-x_L/Puma, liberating p53. Thus, in the modular network of Fig. 1 the release of p53 induces the release of Bax from the complex Bcl2/Bax giving rise to the new complex Bcl2/p53 (Fig. 2b) and unbind Bax forms the Bax/Bax homodimer at the outer membrane of mitochondria. These homodimers may have properties of ionic channels [21]. The rest of the p53 that is not used in the complex can migrate into the nucleus closing a positive loop for Puma production.

In Fig. 3, we transform the molecular steps of Fig. 1 into a chemical kinetics scheme in which we show that there are two sub modules that determine the overall dynamics of the apoptotic response. Even when Puma is not present in the cytoplasm, free cytoplasmic p53 could cause a continuous release of Bax from the complex Bcl2/Bax.

The chemical behaviour of the system in Fig. 4 is mainly due to the k_d values of each complex. Chipuk et al. [9] determined the k_d values for the p53 and Puma complexes with Bcl-x_L as 164 ± 54 nM and 10 ± 4 nM, respectively. Tomita et al. [11] established the k_d value for the Bcl2/p53 complex as 535 ± 24 nM. The value of the k_d of the complex Bcl2/Bax is ~10 nM [19]. According with these data, we model the dynamics of the network using as variables the cytoplasmic concentrations of the complexes Bcl-x_L/p53, Bcl-x_L/Puma, Bcl2/Bax and Bcl2/p53. The temporal change in the concentration of these complexes is given by the set of nonlinear differential equations shown in Table 2. The concentration of the rest of the molecules is also shown in Table 2 and is obtained from the respective algebraic mass balance equation. Initial conditions are referred in Table 3.

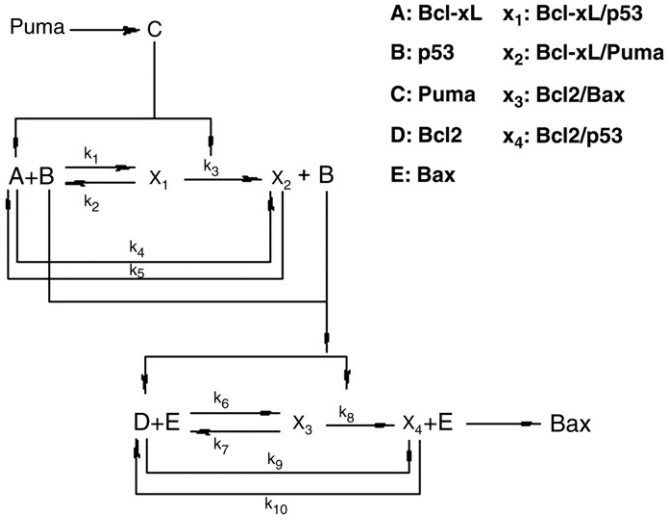

Fig. 3. Schematic representation of the chemical reactions of the sub modules that compose the cytoplasmic apoptotic interaction network of Figs. 1 and 3. In each sub model there are two reversible steps and one irreversible step. p53 protein (B) links both sub modules. The meaning of each variable is given in the upper right corner of the figure. The value of the rate constants is given in Table 3.

We use the RUNGE-KUTTA numerical method to solve this system of equations. We also perform stability analysis to characterize the trajectories and the nature of the equilibrium points of the system in the phase-space. This analysis is used to characterize the robustness of the mathematical model, i.e., the effect of the unknown value of the rate constants of the model on the dynamical behaviour of the system and, as consequence, on the validity of the conclusions obtained from this work. This analysis was performed assigning about 6000 different stochastic values to each unknown parameter and determining the corresponding eigenvalues associated to the Jacobian matrix of the linealized system (see Supplementary material for a more detailed explanation of this procedure). Finally, we perform the bifurcation analysis with respect to the rate constants k_3 and k_8, which control the irreversible steps in the chain of reactions (see Fig. 3), in order to know the possible existence of branched trajectories predicted by the model. These rate constants were varied from 1 to 20 $\mu M^{-1}\ s^{-1}$ (see Supplementary material).

3. Results

3.1. Temporal evolution of the free cytoplasmic Bax concentration in absence and presence of Puma

In order to know the temporal evolution of the system in absence of Puma, we solve the model taking the total cytoplasmic concentration of Puma equal to zero in the set of algebraic mass balance equations of Table 2 (Fig. 4a). This case simulates the activity of p53 in the absence of Puma during the first hour after DNA damage. We extend the time of simulation to two hours covering the total duration of the beginning of the apoptotic process in order to be able to compare the difference in the behaviour of the dynamics of the system in presence and in absence of Puma. From this graph we observe that Bax is released from the Bcl2/Bax complex even in absence of Puma. After two hours Bax reaches ~7.4 nM with a half time $\tau_{500} \approx 2550$ s.

In Fig. 4b we observe the phase plane of free cytoplasmic Bax vs. Bcl-x_L/p53 complex concentration in absence of Puma. In this phase plane the trajectories of the dynamical system clearly show the evolution of the system to a final value of free Bax ~ 10 nM. As expected from Tables 1–3, the initial value of the Bcl-x_L/p53 determines the rate at which Bax is released from its complex with Bcl2. At 0 nM of Bcl-x_L/p53 the system rapidly reaches the attractor point while at 10 nM of Bcl-x_L/p53 the rate is decreased and the system evolves very slowly to the corresponding attractor point. By $t \to 90{,}000$ s all the trajectories have converged to the attractor point (~10 nM, see Supplementary material).

This chemical scenario drastically changes as Puma is released into the cytoplasm. In Fig. 4c we show that at 5 nM of Puma, the final level of free Bax after 2 h is ~8.5 nM, while its $\tau_{500} \approx 45$ s, i.e., 57 times faster than in absence of Puma. As is shown in Fig. 4d, the action of Puma is reflected in the form of the trajectories in the phase plane of free cytoplasmic Bax vs. Bcl-x_L/p53 complex concentration in

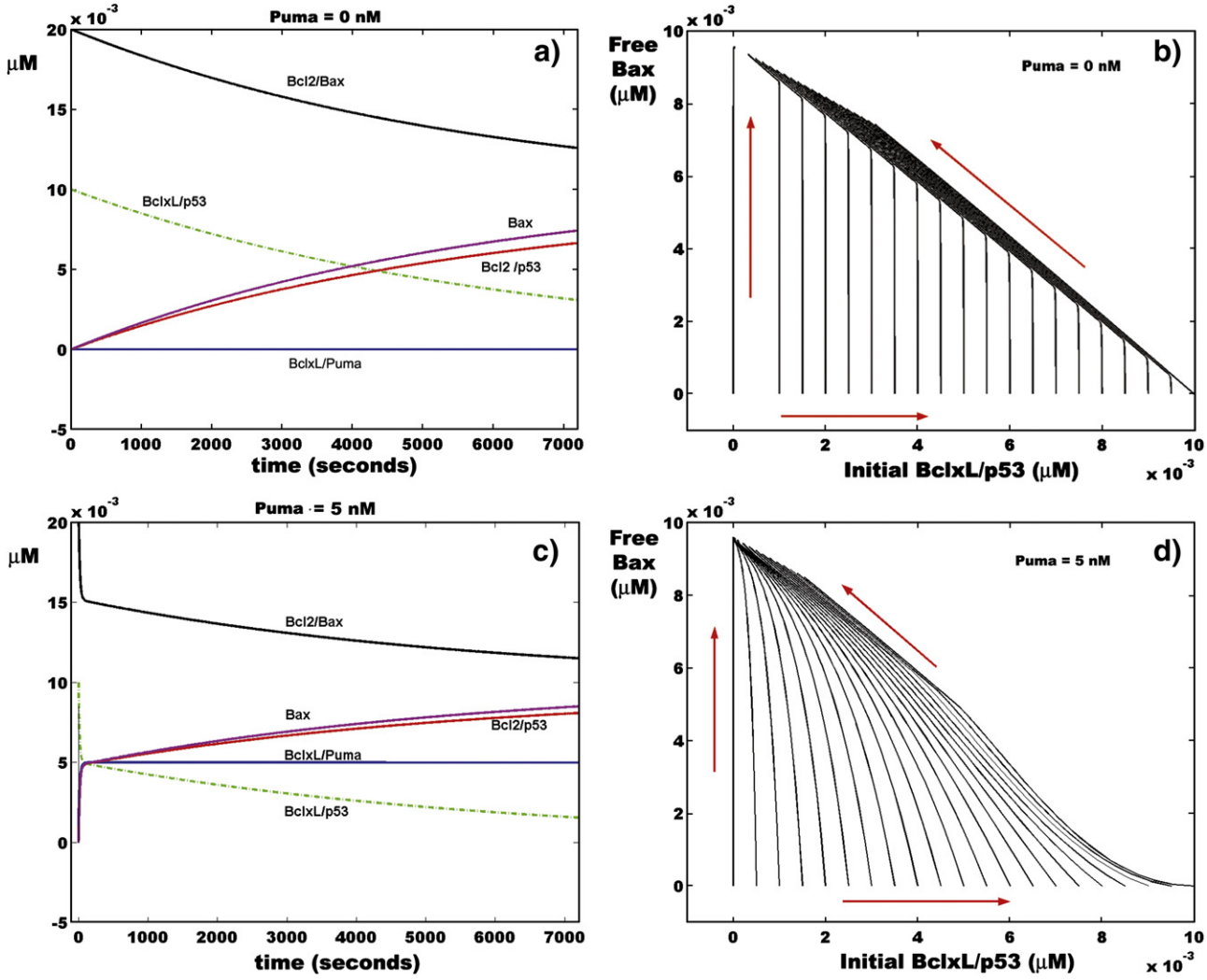

Fig. 4. a) Variation in the concentration of the Bcl-x_L/p53, Bcl-x_L/Puma, Bcl2/p53 and Bcl2/Bax complexes during the time interval of 2 h in the absence of the Puma protein in the cytoplasm. This graph includes the variation of free cytoplasmic Bax concentration. Bax increases its concentration even in the absence of Puma. For this panel, the initial conditions are Bcl-x_L/p53 = 0.01 μM, Bcl-x_L/Puma = 0, Bcl2/p53 = 0 and Bcl2/Bax = 0.02 μM; b) phase plane in which the dependence of the amount of free cytoplasmic Bax on Bcl-x_L/p53 complex initial concentration is shown. The red arrows parallel to each axis indicates the direction of increment of the value of the variables, while the diagonal red arrow indicates the direction in which the trajectories converge into the Bax attractor; c) Variation in the concentration of the Bcl-x_L/p53, Bcl-x_L/Puma, Bcl2/p53 and Bcl2/Bax complexes during the time interval of 2 h in presence of 5 nM of the Puma protein in the cytoplasm. This graph includes the variation of free cytoplasmic Bax concentration. Bax shows a sharp increase in its concentration at the beginning of the Puma discharge into the cytoplasm. For this panel, the initial conditions are Bcl-x_L/p53 = 0.01 μM, Bcl-x_L/Puma = 0, Bcl2/p53 = 0 and Bcl2/Bax = 0.02 μM; d) in presence of 5 nM of Puma the trajectories are deformed with respect to panel (b) indicating a faster Bax liberation from its complex with Bcl2, however the Bax attractor does not change its position in this phase plane (diagonal red arrow indicates the direction in which the trajectories converge into the Bax attractor).

presence of 5 nM of Puma. The trajectories in this new phase plane are distorted with respect to the trajectories shown in Fig. 4b, indicating a faster Bax release from the Bcl2/Bax complex and a faster convergence to the attractor point, which is the same as in Fig. 4b. In this case all the trajectories have converged to the attractor point by $t \rightarrow 25{,}000$ s. From these set of *in silico* experiments, it becomes clear that the role of Puma is to increase the rate at which Bax is released from the complex Bcl2/Bax complex and does not affect the final equilibrium concentration of free cytoplasmic Bax, i.e., Puma affects the rate at which the trajectories drive the system into the attraction basin of the attractor point but it does not change the position of this attractor point in the phase plane of free cytoplasmic Bax vs. Bcl-x_L/p53 complex concentration.

3.2. Stability of the system in the 4D-phase space of the system

Our dynamical system is composed of four nonlinear-coupled differential equations, and its 4D-phase space is defined by the concentrations of the Bcl-x_L/p53, Bcl-x_L/Puma, Bcl2/Bax and Bcl2/p53 complexes. The steady state point or equilibrium point of this dynamical system is reached after 60,000 s (~17 h) in absence of Puma. In order to characterize the stability of this point we allow the system to evolve

Table 1
Chemical reactions of the model.

No	Reactions	Description
1	$p53 + Bcl-x_L \underset{k_2}{\overset{k_1}{\rightleftarrows}} Bcl-x_L/p53$	Bcl-x_L/p53 complex formation
2	$Puma + Bcl-x_L/p53 \xrightarrow{k_3} Bcl-x_L/Puma + p53$	p53 substitution by Puma
3	$Puma + Bcl-x_L \underset{k_5}{\overset{k_4}{\rightleftarrows}} Bcl-x_L/Puma$	Bcl-x_L/Puma complex formation and dissociation
4	$Bax + Bcl2 \underset{k_7}{\overset{k_6}{\rightleftarrows}} Bcl2/Bax$	Bcl2/Bax complex formation and dissociation
5	$p53 + Bcl2/Bax \xrightarrow{k_8} Bcl2/p53 + Bax$	Bax substitution by p53
6	$p53 + Bcl2 \underset{k_{10}}{\overset{k_9}{\rightleftarrows}} Bcl2/p53$	Bcl2/p53 complex formation and dissociation

Table 2
Algebraic and differential equations of the model.

$\frac{d[p53/Bcl-x_L]}{dt} = J_1 - J_2 - J_3$	$J_1 = k_1 \cdot [p53] \cdot [Bcl\text{-}x_L] - k_2 \cdot [p53/Bcl\text{-}x_L]$
$\frac{d[Puma/Bcl-x_L]}{dt} = J_2 + J_3$	$J_2 = k_3 \cdot [Puma] \cdot [Bcl\text{-}x_L]$
$\frac{d[Bax/Bcl2]}{dt} = J_4 - J_5 - J_6$	$J_3 = k_4 \cdot [Puma] \cdot [Bcl\text{-}x_L] - k_5 \cdot [Puma/Bcl\text{-}x_L]$
$\frac{d[p53/Bcl2]}{dt} = J_5 + J_6$	$J_4 = k_6 \cdot [Bax] \cdot [Bcl2] - k_7 \cdot [Bax/Bcl2]$
	$J_5 = k_8 \cdot [p53] \cdot [Bax/Bcl2]$
$[Bcl\text{-}x_L] = [Bcl\text{-}x_L]_T - ([p53/Bcl\text{-}x_L] + [Puma/Bcl\text{-}x_L])$	$J_6 = k_9 \cdot [p53] \cdot [Bcl2] - k_{10} \cdot [p53/Bcl2]$
$[Bcl2] = [Bcl2]_T - ([Bax/Bcl2] + [p53/Bcl2])$	
$[p53] = [p53]_T - ([p53/Bcl\text{-}x_L] + [p53/Bcl2])$	
$[Puma] = [Puma]_T - [Puma/Bcl\text{-}x_L]$	
$[Bax] = [Bax]_T - [Bax/Bcl2]$	

from the initial condition set $x_0 = [0.01\ 0\ 0.02\ 0]^T$ (μM) for the respective complexes above. The final fixed point is $x^0 = [0.00003\ 0\ 0.01\ 0.0094]^T$ (μM) in the absence of Puma. The Jacobian matrix (**J**) of the linearized set of equations around x^0 has eigenvalues $\lambda_i < 0$, $i = 1,2,3,4$. These eigenvalues mean that the fixed point attained by the system in its 4D-phase space in the absence of Puma is asymptotically stable (see Supplementary material), i.e., it is an attractor.

According to this result, in the *absence of Puma* the system reaches a stable fixed point in which the concentration of Bcl-x_L/p53 varies from 10 to ~0.03 nM, the concentration of Bcl-x_L/Puma is always 0 nM, the concentration of the Bcl2/Bax complex varies from 20 nM to ~10 nM and the concentration of the complex Bcl2/p53 varies from 0 to ~9.4 nM.

By contrast, in presence of 5 nM of Puma the fixed point or equilibrium point of this dynamical system is reached after 25,000 s (~7 h). In order to characterize the stability of this point we allow the system to evolve from the initial condition set $x_0 = [0.01\ 0\ 0.02\ 0]^T$ (μM) for the respective above complexes. The final fixed point is $x^0 = [0.00005\ 0.004\ 0.01\ 0.0095]^T$ (μM). The Jacobian matrix (**J**) of the linearized set of equations around x^0 also has eigenvalues $\lambda_i < 0$, $i = 1,2,3,4$. These eigenvalues mean that the fixed point attained by the system in its 4D-phase space in presence of 5 nM of Puma is also asymptotically stable (see Supplementary material), i.e., it is an attractor.

According to this result, in the presence of 5 nM of Puma the system reaches a stable fixed point in which the concentration of Bcl-x_L/p53 varies from 10 to ~0.05 nM, the concentration of Bcl-x_L/Puma varies from 0 to ~4 nM, the concentration of the Bcl2/Bax complex varies from 20 nM to ~10 nM and the concentration of the complex Bcl2/p53 varies from 0 to ~9.5 nM.

The bifurcation analysis with respect to parameters k_3 and k_8 does not show the existence of branched trajectories for free Bax concentration, i.e., the 4D-phase space for our dynamical system is characterized by a single stable fixed point in which all the trajectories converge.

However, k_9 sets a bifurcation point at 0.017 $\mu M^{-1} s^{-1}$ for which the dynamical system steady state is stable if $k_9 \leq 0.017$ and unstable otherwise. This result is important because this rate constant indirectly controls the dissociation rate of the Bcl2/Bax complex [19] (see Supplementary material). In this work we used the value of 0.01 $\mu M^{-1} s^{-1}$ for this parameter, which ensures the stability of the dynamical system.

3.3. Effect of Puma on free cytoplasmic Bax concentration

In other set of *in silico* experiments we simulate the effect of the Puma protein concentration as it is been released into the cytoplasm after a severe DNA damage. In this case the initial condition for each complex was taken as a constant and we vary the total amount of cytoplasmic Puma from 0 to 5 nM after a time lag of 3600 s in which we assume that the Puma protein is beginning to be released into the cytoplasm after its translation [9]. We use the function $puma(t) = puma^{max}\ (1 - e^{-\alpha(t-3600)})$ to simulate the increase of Puma cytoplasmic concentration, where $puma^{max}$ is the maximum level of Puma (assumed to be 5 nM) and α is the intrinsic rate of variation of Puma cytoplasmic concentration.

Fig. 5a we show the effect of Puma on the free cytoplasmic concentration of Bax after the time lag of 3600 s. Puma increases the rate at which free Bax reaches its attractor point, but does not change the position of this point, as expected. Fig. 5b we show the effect of varying α and, as expected, when the value of this parameter is increased the rate at which Bax reaches its maximum concentration is also increased.

3.4. Effect of different initial concentrations of Bcl2/Bax complex on free Bax–free p53 cytoplasmic equilibrium

In Fig. 6 we show the effect of different initial concentrations of Bcl2/Bax complex on the value of the ratio $r = \frac{\text{Free Cytoplasmic Bax}}{\text{Free Cytoplasmic p53}}$. In this *in silico* experiment, we allow the system evolve during an interval of time of approximately 10 h from an initial state in absence of Puma to a final state in presence of 5 nM of Puma. The release of Puma into de cytoplasm was simulated using the same function of the preceding Section 3.3, with an $\alpha = 0.001975\ s^{-1}$.

Table 3
Parameters of the model.

Parameters	Description	Value	References
$[p53]_T$	Total concentration of p53	0.01 μM	Estimated from [9]
$[Bcl\text{-}x_L]_T$	Total concentration of Bcl-x_L	0.01 μM	Estimated from [9]
$[Puma]_T$	Total concentration of Puma	0–0.005 μM	Control variable
$[Bax]_T$	Total concentration of Bax	0.02 μM	Estimated from [10]
$[Bcl2]_T$	Total concentration of Bcl2	0.03 μM	Same as in [10]
$[Bcl\text{-}x_L/p53]_0$	Initial concentration of Bcl-x_L/p53	0.01 μM	Used in this work
$[Bcl\text{-}x_L/Puma]_0$	Initial concentration of Bcl-x_L/Puma	0 μM	Used in this work
$[Bcl2/Bax]_0$	Initial concentration of Bcl2/Bax	0.02 μM	Used in this work
$[Bcl2/p53]_0$	Initial concentration of Bcl2/p53	0 μM	Used in this work
k_1	Dimerization between p53 and Bcl-x_L	0.001 $\mu M^{-1}\ s^{-1}$	Estimated from k_d [9]
k_2	Dissociation of Bcl-x_L/p53	0.000164 s^{-1}	Estimated from k_d [9]
k_3	Puma displaces p53 from Bcl-x_L/p53	10 s^{-1}	Stability analysis is performed
k_4	Dimerization between Puma and Bcl-x_L	0.005 $\mu M^{-1}\ s^{-1}$	Estimated from k_d [9]
k_5	Dissociation of Bcl-x_L/Puma	0.00005 s^{-1}	Estimated from k_d [9]
k_6	Dimerization between Bax and Bcl2	0.001 $\mu M^{-1}\ s^{-1}$	Estimated from k_d [19]
k_7	Dissociation of Bcl2/Bax	0.00001 s^{-1}	Estimated from k_d [19]
k_8	p53 displaces Bax from Bcl2/Bax	10 s^{-1}	Stability analysis is performed
k_9	Dimerization between p53 and Bcl2	0.01 $\mu M^{-1}\ s^{-1}$	Estimated from k_d [11]
k_{10}	Dissociation of Bcl2/p53	0.535 s^{-1}	Estimated from k_d [11]

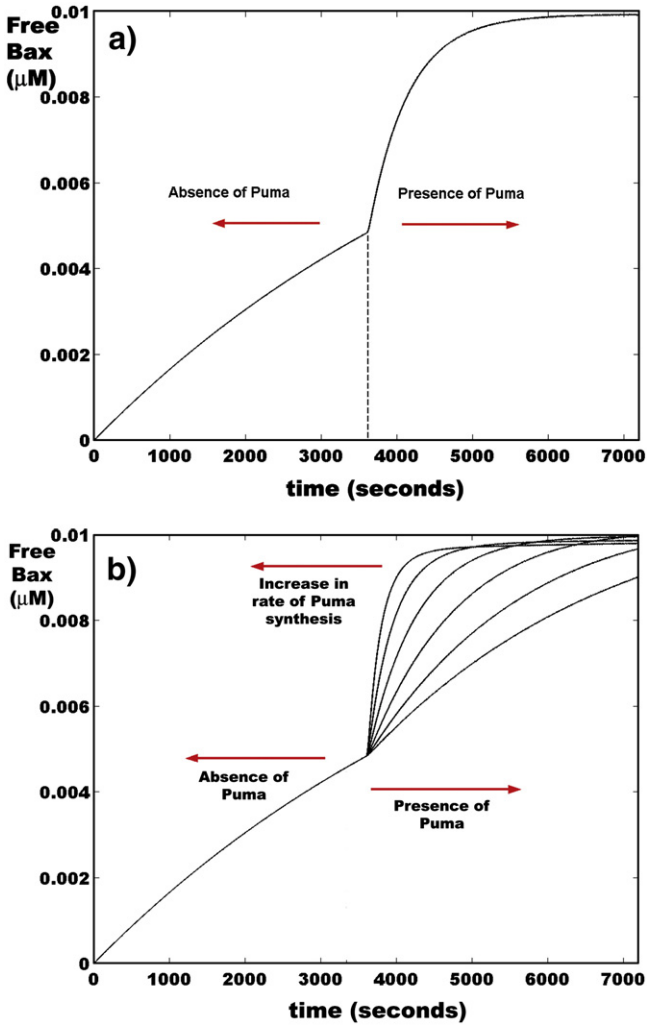

Fig. 5. a) *In silico* experiment in which the dynamical system is allowed to evolve in absence of Puma during the first 3600 s and then the release of Puma into the cytoplasm after its translation is simulated by the function $\text{puma}(t) = \text{puma}^{\max}\,(1 - e^{-\alpha(t-3600)})$ with $\alpha = 0.001975\ s^{-1}$. According to this function, Puma reaches a concentration value of 5nM in the time interval from 3601 to 7200 s. This panel shows that the presence of Puma accelerates the process of liberation of Bax, allowing a maximum value of ~10 nM of free cytoplasmic Bax to be reached in ~3000 s after Puma started to be released into the cytoplasm; b) *in silico* experiment in which the parameter α of the function of panel (a) varied from 0.00001975 to 0.001975 s^{-1}. The release of Bax from its complex is faster as α is increased, but the Bax attractor is not altered. The initial conditions for each panel are Bcl-x_L/p53 = 10 nM; Bcl-x_L/Puma = 0 nM; Bcl2/Bax = 20 nM; Bcl2/p53 = 0 nM.

As indicated in Table 1, the concentration of free cytoplasmic Bax and free cytoplasmic p53 can be calculated as:

$$[\text{Bax}] = [\text{Bax}]_T - [\text{Bcl2}/\text{Bax}]$$

$$[\text{p53}] = [\text{p53}]_T - ([\text{Bcl} - \text{x}_\text{L}/\text{p53}] + [\text{Bcl2}/\text{p53}])$$

thus, r is given by:

$$r = \frac{[\text{Bax}]}{[\text{p53}]} = \frac{[\text{Bax}]_T - [\text{Bcl2}/\text{Bax}]}{[\text{p53}]_T - ([\text{Bcl} - \text{x}_\text{L}/\text{p53}] + [\text{Bcl2}/\text{p53}])}$$

According to this equation, free p53 concentration depends on two factors, assuming that the total amount of p53 in the cytoplasm is relatively constant during the experiment: a) the concentration of the Bcl-x_L/p53 complex at a given time and b) the concentration of the Bcl2/p53 complex at the same instant of time.

In contrast, free Bax concentration depends only on the concentration of the Bcl2/Bax complex, assuming that the total amount of Bax in the cytoplasm is relatively constant during the experiment.

Fig. 6a shows the evolution of the dynamical system projected on the Bax vs. p53 phase plane. Each trajectory corresponds to a different initial Bcl2/Bax concentration. As observed, the amplitude of the trajectories decreases as the initial concentration increases but all of them converge to a fix point for which [p53] ≈0.6 nM and [Bax] ≈10 nM.

At low complex concentrations most of the Bax (≈20 nM) and Bcl2 (≈30 nM) are initially free while most of p53 is bound to Bcl-x_L. Under this circumstance, according with our model results, Bax remains free during the first 10,000 s (~2.5 h) of the dynamics while p53 has begun its chemical interaction with Bcl2, forming half of the Bcl2/p53 final concentration (≈9 nM) in approximately 8000 s

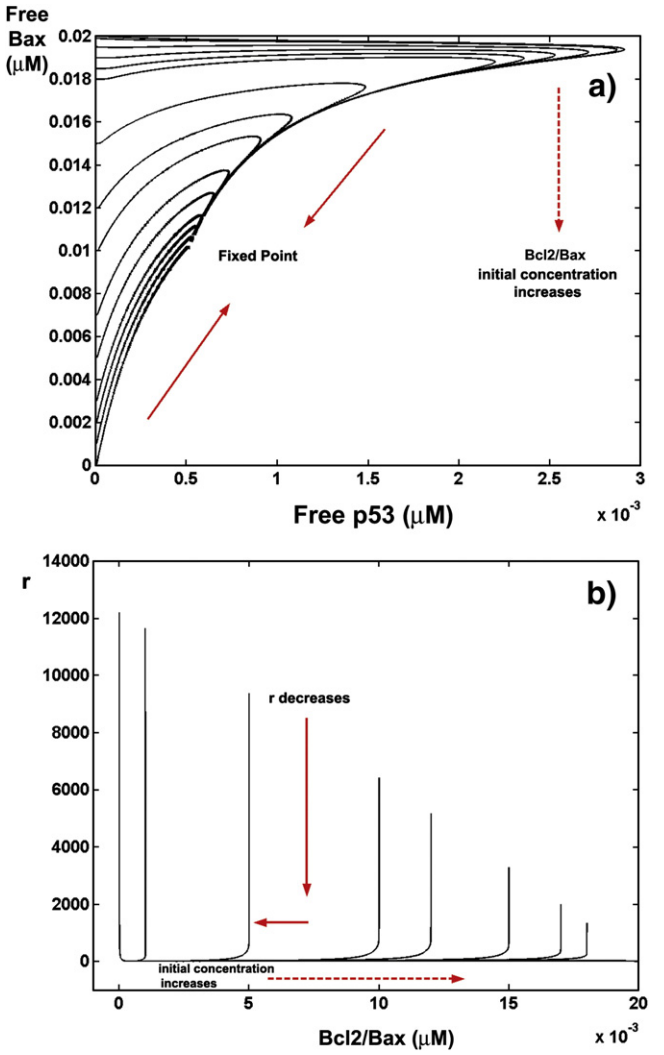

Fig. 6. *In silico* experiment in which the dynamical system is allowed to evolve in absence of Puma during the first 3600 s and then the release of Puma into the cytoplasm after its translation is simulated by the function $\text{puma}(t) = \text{puma}^{\max}\,(1 - e^{-\alpha(t-3600)})$ with $\alpha = 0.001975\ s^{-1}$. (a) Bax vs p53 phase plane in which the corresponding trajectories to different initial concentrations of the Bcl2/Bax complex are shown. The amplitude of the trajectories decreases as the complex initial concentration increases. After 36000 s all of them have converged into a fixed point for which free Bax concentration ≈10 nM and free p53 concentration ≈0.6 nM. Continuous red arrows indicate the convergence direction of the trajectories; b) Free Bax–free p53 ratio (r) vs. initial concentration of the Bcl2/Bax complex. Continuous red arrows indicate the convergence direction of the trajectories to the value $r \approx 16.66$. The initial conditions for the rest of the complexes are Bcl-x_L/p53 = 10 nM; Bcl-x_L/Puma = 0 nM; Bcl2/p53 = 0 nM. The total amount of cytoplasmic Bax and p53 are 20 nM and 10 nM respectively (see Table 3).

(~2 h). In contrast, Bcl2/Bax reaches half of its final value (≈10 nM) in 35,000 s (~10 h). In this form, the presence of Puma accelerates the liberation of p53 from the Bcl-x_L/p53 complex, and free p53 binds to Bcl2 faster than Bax, increasing the time in which Bax remains free. If we block the formation of the Bcl2/p53 complex ($k_8 = 0$) the Bcl2/Bax reaches half of its final value (12 nM) in only 15,000 s (~4 h) in presence of Puma.

In contrast, when the initial concentration of Bcl2/Bax is 10 nM, the system dynamics is very fast, as described in Section 3.3 of Results section, giving rise to very short and straight trajectories that converge into the fixed point.

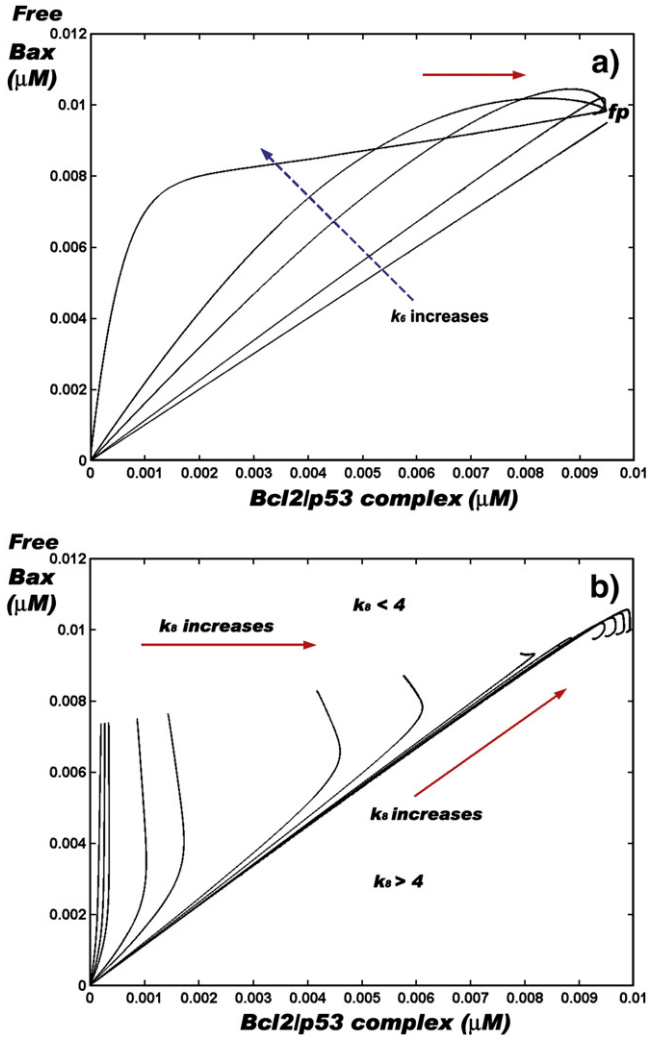

Fig. 7. *In silico* experiment in which the dynamical system is allowed to evolve in absence of Puma during the first 3600 s and then the release of Puma into the cytoplasm after its translation is simulated by the function $\text{puma}(t) = \text{puma}^{\max}(1 - e^{-\alpha(t-3600)})$ with $\alpha = 0.001975\ s^{-1}$. (a) Free Bax vs Bcl2/p53 phase plane in which the corresponding trajectories to different values of the parameter k_6 are shown. The amplitude of the trajectories increases as the k_6 varies from 0.0001 to 0.1 $\mu M^{-1}s^{-1}$. After 36000 s all of them have converged into a fixed point (fp) for which free Bax concentration ≈10 nM and Bcl2/p53 concentration ≈10 nM. (b) Free Bax vs Bcl2/p53 phase plane in which the trajectories corresponding to different values of the parameter k_8 are shown. For $k_8 < 4$ $\mu M^{-1}s^{-1}$, the trajectories increases their amplitude as the parameter values changes from 0.001 to 3 $\mu M^{-1}s^{-1}$. Each trajectory drives the system into a particular fixed point. For $k_8 \geq 4$ $\mu M^{-1}s^{-1}$, the trajectories are packaged into a narrow zone of the phase plane and drive the system to different fixed points that conform a compact attraction basin for the dynamical system. In this panel k_8 was varied from 4 to 20 $\mu M^{-1}s^{-1}$. In both panels the continuous red arrow indicates the convergence direction of the trajectories. The initial conditions for the complexes are Bcl-x_L/p53 = 10 nM; Bcl-x_L/Puma = 0 nM; Bcl2/Bax = 20 nM; Bcl2/p53 = 0 nM (see Table 3).

In all cases the final value of r is 16.66 that implies that the system reaches a steady state in which the amount of free Bax is ~17 times greater than free p53 in presence of Puma. In this steady state, most of the p53 is part of the Bcl2/p53 complex (≈9.4 nM), and only a relatively small fraction (≈0.025 nM) is part of the Bcl-x_L/p53 complex.

Fig. 6b shows a more detailed view of this dynamic feature of the system. At low initial Bcl2/Bax concentration the value of r is initially high because the amount of free p53 is relatively low and the amount of free Bax is high. At steady state r falls to 16.66 because only half of the total amount of Bax remains free, while most of p53 is now attached to Bcl2 (see Fig. 1).

At high initial Bcl2/Bax concentration there is practically no free Bax and the value of r is relatively small. At steady state free Bax has been increased to ~10 nM due to its substitution by p53 (in presence of Puma) from the Bcl2/Bax complex (see Fig. 1) and $r \approx 16.66$. These results show the insensitivity of the dynamical system to the initial concentration of Bcl2/Bax, which is reflected in the fact that r final value is independent of the trajectory followed to it.

3.5. Effect of variations in parameter k_6 on the Free Bax vs. Bcl2/p53 equilibrium

Parameters k_6 and k_7 govern the association ↔ dissociation dynamics between the anti-apoptotic Bcl2 and the pro-apoptotic Bax proteins in cytoplasm (see Fig. 3 and Table 1). These parameters are related by their respective k_d value (see Table 3). Thus, it is necessary to vary only k_6 to understand how the equilibrium Bax ↔ Bcl2/Bax is altered, assuming that the rest of the parameters remain constants.

However, Bcl2/Bax can be also removed from the system by substitution of Bax by p53 (See Fig. 3). Thus, we measure the effect of k_6 on the Bax–Bcl2/p53 equilibrium instead of the Bax–Bcl2/Bax balance to understand how this parameter influences the final step in the series of kinetic equations shown in Fig. 3, which leads to the delivery of Bax in the neighbourhood of the mitochondria.

The presence of Puma in the system was modeled as in Section 3.4 of Results section, and the set of differential equations of the model equations was numerically solved allowing time to reach 36000 s (10 h) for which all the trajectories have converged to the fixed point. We assume that the total amount of p53, Bcl2, Bax and Bcl-x_L remain reasonably constant during this time interval.

In Fig. 7a, k_6 is systematically varied from ~0 to 0.1 $\mu M^{-1}\,s^{-1}$ (only some trajectories are shown). At the end of the 10 h., all the trajectories have converged to a fixed point in the Free Bax vs. Bcl2/p53 phase plane, for which [Bax]~10 nM and [Bcl2/p53] ~10 nM. Thus, the value of k_6 has not effect on the final fixed point reached by the system.

However, k_6 influences the form of the trajectory followed by the dynamical system during its temporal evolution. The k_d for the Bcl2/Bax complex is ~10 nM [19] and it is sustained as a constant during this experiment. Thus, as the k_6 value increases Bcl2 and Bax tend to form the Bcl2/Bax complex in a faster form, possibly hindering the substitution of Bax by p53. The result is that the dynamical system follows a larger trajectory to the fixed point in which all the Bax could be finally substituted by p53 from its complex with Bcl2.

3.6. Effect of variations in parameter k_8 on the free Bax vs. Bcl2/p53 equilibrium

Parameter k_8 governs the rate of substitution of Bax by p53 from its complex with Bcl2. In our model, we assume that this step is practically irreversible because free Bax tends to rapidly form the Bax/Bax homodimer at the mitochondria membrane [11,21].

In this *in silico* experiment, the presence of Puma in the system was modeled in the same form as in Section 3.4. We varied k_8 from

0.001 to 20 $\mu M^{-1}s^{-1}$ and the set of differential equations of the model equations was numerically solved as before. We assume that the *total* amount of p53, Bcl2, Bax and Bcl-x_L remain reasonably constant during the experiment.

The parameter k_8 cleavages the Free Bax vs. Bcl2/p53 plane into two regions, depending on its value. For $k_8<4$ $\mu M^{-1}s^{-1}$ the trajectories are grouped when $k_8<1$ and become of major amplitude when $k_8>1$. In all cases, each one tends to reach a particular fixed point for which free Bax concentration ranges from ~7.5 to 9 nM, while Bcl2/p53 concentration ranges from ~0.2 to 8 nM. The time required to converge to each fixed point increases as k_8 decreases, and all of the trajectories have converged to its respective attractor at the end of 108,000 s (~30 h).

For $k_8 \geq 4$ $\mu M^{-1}s^{-1}$ all trajectories are packaged into a narrow region of the phase plane and converge to different fixed points that conform a compact attraction basin for the dynamical system (Fig. 7b), in which Free Bax concentration ranges from ~9.5 to 10 nM and Bcl2/p53 complex ranges from ~9 to 10 nM. The time required to converge to each fixed point increases as k_8 decreases, but in this case all of the trajectories have converged into its respective fixed point at the end of ~35,000 s.

From these results is clear that parameter k_8 controls the rate of the final output of the dynamical system in presence of Puma and that the system can converge into different fixed points with different velocities. However, the free Bax concentration varies in a narrow interval of values from ~7.5 to 10 nM, while Bcl2/p53 varies in a wider interval of values from ~0.2 to 10 nM, indicating that the presence of Free Bax in the system depends mainly on the value of the k_d for its binding with Bcl2 and that, under genotoxic damage conditions, p53 accelerates the Bax release process in presence of Puma, assuming that the rest of the parameters remain constants (see Fig. 3).

4. Discussion

Several proteins involved in DNA repair show a 'dot-like' localization, which can be modulated by ionizing radiation (IR) [22]. Different factors implicated in repair of double strand breaks (DSB), co-localize with promyelocytic leukaemia protein (PML). For example, the repair proteins Rad51 and MRN form dots in unstressed cells, and IR increases the number of such structures, designated IR-induced foci (IRIF). Despite the similar appearance, but consistent with partially different functions, Rad51 and MRN seem to form over-lapping domains [22]. In irradiated cells, Rad51 localize within domains that overlap with sites of DNA breaks, underlying the importance of PML as a scaffold for these IRIF. These sites might represent irreparable or slowly repaired lesions. p53 was also identified at the same sites. The presence of p53 within such structures could be required to transmit the signal for blocking cell cycle progress until all lesions have been repaired.

As we mentioned before, DNA repairing after IR damage implies the presence of a nuclear ATM molecular switch that give rise to a low frequency limit cyclic via a Hopf supercritical bifurcation [8,14,15]. It has been suggested that this cycle could be a persistent mechanism that is periodically reinforced to ensure the complete repair of the damage. In this form, nuclear oscillations of the p53-Mdm2 system could act a timer control for events like cell cycle arrest and apoptosis. Puma, Bax and other pro-apoptotic genes can be driven to express in each cycle up to reach a threshold value to activate apoptosis if necessary [15].

In contrast, our results show that in the cytoplasm, during the first two hours after IR damage, the global dynamical behaviour of the net of Fig. 3 is characterized by the existence of converging trajectories into a steady attractor.

After DNA injure, part of the pool of cytoplasmic p53 is transported into the nucleus and the rest is directed to the mitochondria neighbourhood where it forms the Bcl-x_L/p53 complex. In the absence of Puma the presence of free cytoplasmic p53 drives a continuous and slow leak of Bax from the Bcl2/Bax pool (see Figs. 1, 2b and 3). As we pointed out in the Results section, this process is strongly dependent on the initial amount of free p53 present in cytoplasm (Fig. 4a and b).

However, Bax always reaches a steady value of ~10 nM after 60,000 s, in absence of Puma, indicating that this leak is a structural feature of the interaction network (Figs. 1 and 3). The presence of a lag between the onset of the DNA damage and the activation of the caspase 9 has been reported in [5]. This lag has duration of approximately 10 min and in this time our model reports an increase in free Bax concentration of only ~1.5 nM, assuming that initially all the Bax is bounded to Bcl2 and Puma is not still present in the cytoplasm (see Fig. 5a). Thus, there is the possibility that for the initiation of the apoptotic process is not necessary a great amount of free Bax [9,17–19] and that a small quantity of this pro-apoptotic molecule is enough to produce the initial threshold number of Bax/Bax homodimers and Bax/Bak heterodimers at the mitochondria membrane to start the release of cytochrome c.

This slow p53-driven liberation of Bax from its complex with Bcl2 could be a mechanism that allows the cell to repair the DNA damage while Puma protein begins to be expressed in the cytoplasm. If the DNA damage cannot be repaired then the phosphorylated form of p53 induces the transcription of Puma and other pro-apoptotic genes, driving cell death as soon as possible. In this work we assume that the initial production of Puma takes about an hour since the moment DNA damage induces the activation of the ATM kinase in the nucleus [23].

In this interval of time free cytoplasmic Bax reaches a value of ~6 nM (Fig. 5a). The presence of Puma behaves like a switch and accelerates this process of liberation of Bax from its complex. Then, the pro-apoptotic protein reaches its steady concentration of ~10 nM in a few minutes, depending on the intrinsic rate of variation of Puma cytoplasmic concentration (α) [18] (Figs. 4c and 5a).

According to the set of chemical equations of the network (Fig. 3), Puma cleavages the Bcl-x_L/p53 complex increasing the levels of free cytoplasmic p53, driving the overall equilibrium of the chemical system towards a faster liberation of Bax (Fig. 5b) [9] without relocating the fixed point in the phase plane of Bax vs Bcl-x_L/p53 initial concentration (Fig. 4d) but deforming the original trajectories to this point (Figs. 4d and 5b). These in silico experiments support the idea that the role of Puma is to increase the rate at which the free cytoplasmic concentration of Bax reaches its maximum value but not to affect this maximum value itself.

This switch like dynamical behaviour of the net of chemical processes that leads to cell death has been reported in other works, principally by [18] that suggests the existence of a "Bcl2 switch" upstream the mitochondria.

In accordance with [18], from our model emerges a dynamical scenario in which, during the first hour, the intrinsic slow p53-driven free Bax increment in the cytoplasm produces the instability of the net of pro-apoptotic processes that leads the dynamical system into a transitory "saddle-like" point at the threshold Bax concentration of ~5 nM. From this moment, the presence of Puma switches the Bax concentration into its maximum value in a few minutes, driving the system's trajectory to a stable fixed point that correspond to the consequent irreversible cell death [5,17–19].

Fig. 6 shows this effect in a clearer form, taking the initial concentration of the Bcl2/Bax complex as a control variable. In Fig. 6a all the trajectories of the system converges into the same fixed point under the continuous release of Puma into the cytoplasm (see Sections 3.3 and 3.4 of the Results section), independently of the initial concentration of the Bcl2/Bax complex. However, at low initial Bcl2/Bax concentrations the amplitude of the trajectories is larger, which is an important property of the net of Fig. 3 because reflects the fact that initial high concentrations of Bax can be regulated in presence of high concentrations of Bcl2, but this control process

occurs in a slow form due to the faster interaction of free p53 (released from the Bcl-x_L/p53 complex by Puma) with Bcl2 that competitively blocks the binding of Bax with Bcl2 (see Section 3.4 in the Results section).

This regulatory feature of the net of chemical reactions (Fig. 3) are represented, in our model, by the free Bax–free p53 ratio (r) value. All the trajectories converge to the ratio number 16.66 when the initial concentration of Bcl2/Bax is varied (Fig. 6b), i.e., $r = 16.66$ means cell death in this case. Although each trajectory represents a different temporal evolution of the system in the Bax vs. p53 phase plane, all of them converge to the attractor point from which this r value is settled down. Thus, this result also implies that in the basin of attraction of the fixed point, the dynamical system is asymptotically stable against small perturbations in the steady Bcl2/Bax concentration, once Puma has reached its steady maximum value of 5 nM (see below). This *in silico* experiment indicates that other possible effect of Puma is to increase the time at which initial high concentrations of free Bax remain before Bcl2 can down regulate them.

Previous works on the modeling of apoptosis [17,18] have not considered the modularity of the network of interaction between the complex of p53 and Puma with the anti-apoptotic protein Bcl-x_L and p53, and of Bax with the anti-apoptotic protein Bcl2. This network has interesting topological properties (Fig. 2) because it has a high degree of auto-organization into a functional unity that implies that the change in the concentration of any of its components will produce a concomitant change in the concentration of the rest. The dynamical behaviour of the net in its 4D-phase space, in presence and absence of Puma, is represented by its evolution to an asymptotically stable fixed point whose position in the phase space changes depending only on the presence or absence of the Bcl-x_L/Puma complex, for the particular set of parameter values in Table 3. Furthermore, the presence of Puma provoke that some of the eigenvalues acquire a more negative value as the perturbed parameters increase their values (see Supplementary material). Thus all the trajectories in the attraction basin of this point will be attracted by it, indicating that the pro-apoptotic process is quite irreversible once Puma is released into the cytoplasm. As consequence, the network is also robust against perturbations in the value of the rate constants if $k_9 \leq 0.017\ \mu M^{-1}s^{-1}$ (see Supplementary material).

As we mentioned before, variations from 1 to 20 $\mu M^{-1}s^{-1}$ in the key parameters k_3 and k_8, that determines the rate of the irreversible steps of the set of chemical reactions (Fig. 3), do not affect the stable dynamical behaviour of the network and no branched trajectories could be located in presence of a constant concentration of 5 nM of Puma for the particular value of the parameter k_9 used in this work (see Table 3 and Supplementary material). Thus, for the set of parameter values of our model we do not expect sudden changes in the dynamical behaviour of the net and this characteristic increases the confidence on the fact that the slow liberation of Bax in absence of Puma is a structural feature of the network, result of the combination of the values of the k_d's reported in Table 3.

Interesting additional properties of the dynamical system arise as consequence of the variation of the parameters k_6 and k_8 values under a continuous release of Puma into the cytoplasm modeled by the function $\text{puma}(t) = \text{puma}^{\max}\ (1 - e^{-\alpha(t-3600)})$ (see Sections 3.3, 3.5 and 3.6 of the Results section).

From Fig. 7a is clear that parameter k_6 has not influence in the localization of the fixed point in the Bax vs. Bcl2/p53 phase plane of the dynamical system but influences the form of the trajectories. If this parameter is varied from 0.0001 to 0.1 $\mu M^{-1}s^{-1}$ the trajectories are deformed and they become larger as k_6 increases its value. k_6 determines the rate of formation of the Bcl2/Bax complex (see Table 1 and Fig. 3). Thus, its increment shifts the direction of the reaction to the formation of the complex by a faster binding of Bax by Bcl2. As we mentioned before, for the particular value of k_6 shown in Table 3, Bcl2 binds p53 faster than Bax. Consequently, any increment in the value of this parameter introduces a delay in the substitution of Bax by p53 and enlarges the trajectory without affecting the final equilibrium point. In other words, the output of the dynamical system, free Bax, reaches the same level but in a larger time as k_6 is increased in conjunction with the release of Puma into the cytoplasm.

Systematic variation of parameter k_8 value splits the Bax vs. Bcl2/p53 phase plane into two well define regions (Fig. 7b). This parameter determines the rate of the irreversible chemical substitution of Bax by p53 from the Bcl2/Bax complex. Low rates of this process ($k_8 < 4\ \mu M^{-1}s^{-1}$), in conjunction with the continuous release of Puma into the cytoplasm, produce a series of trajectories that lead to different fixed points. However, the difference between the lowest and highest free Bax concentration in this zone is only ~1.5 nM. In contrast, high rates of Bcl2/p53 formation ($k_8 \geq 4\ \mu M^{-1}s^{-1}$) produces a set of trajectories packed into a narrow zone of the phase plane that leads to different attracting points, for which free Bax concentration ranges from ~9.5 nM to 10 nM and Bcl2/p53 concentration ranges from ~9.4 nM to 10 nM. For the particular value of $k_8 = 10\ \mu M^{-1}s^{-1}$ the final free Bax concentration coincides with the value mentioned in Section 3.3 of the Results sections (~10 nM) when Puma reaches the steady value of 5 nM. In this form the key parameter k_8 determines both the velocity of the Bcl2/p53 formation and the localization of the fixed point of the dynamical system under a continuous release of Puma into the cytoplasm.

5. Conclusion

The apoptotic process is a cellular mechanism that avoids that cells with severe DNA damage can survive and divide propagating the somatic damage to their daughter cells [1–3]. The modification of the chromatin (deletion, insertions, punctual mutations, among others possible injury processes) by stress is sensed by the ATM kinase system [22], which phosphorylates a steady pool of the p53 transcription factor. Phosphorylated p53 induces the transcription of a series of downstream pro-apoptotic genes including *Puma*. The latter codes for its protein, that interacts with the Bcl-xL family of anti-apoptotic cytoplasmic proteins [9].

The pool of free p53 that remains at the cytoplasm induces the liberation of Bax at a low rate even in absence of the Puma. According to our results, the possible biological significance of this process may be to allow a lag between the starting of the DNA damage repair process and the onset of the full apoptotic process when the damage cannot be repaired in a pre-set moment of the cell cycle, in which Puma reaches a threshold concentration value that fires the complete and irreversible apoptotic process.

From a dynamical point of view the stability and robustness of the network of interaction between p53 and the pro and anti-apoptotic proteins BclxL, Bcl2, Puma and Bax ensures that the corresponding 4D-phase space, represented by our dynamical system of Table 2, is characterized by the existence of converging trajectories into a steady attractor and that this flow is reasonably independent of the values assigned to the rate constants. This property of the network is what allows us to have a great confidence in the fact that the predicted continuous p53-driven liberation of Bax from the Bax/Bcl2 complex is a real structural feature of the network components interactions and not a fake property of it.

Acknowledgments

We thank Dr. Ramón González, from the Adenovirus Laboratory of the Facultad de Ciencias of the Universidad Autónoma del Estado de Morelos for his interesting discussions and suggestions about the content of this work. We also thank Dra. Nina Pastor, from the Molecular Biophysics Group of the same University by her interesting suggestions and corrections to the content of this paper. Both authors of this work were supported by the grant PROMEP/103.5/07/2674.

Appendix A. Supplementary data

Supplementary data associated with this article can be found, in the online version, at doi:10.1016/j.bpc.2009.03.012.

References

[1] Bert Vogelstein, Kenneth W. Kinzler, Cancer genes and the pathways they control, Nature Medicine 10 (2004) 789–799.
[2] Hitoshi Okada, Tak W. Mak, Pathways of apoptotic and non-apoptotic death in tumour cells, Nature Reviews/Cancer 4 (2004) 592–603.
[3] Susan Haupt, Michael Berger, Zehavit Goldberg, Ygal Haupt, Apoptosis — the p53 network, Journal of Cell Sciience 116 (2003) 4077–4085.
[4] Chris J Norbury, Boris Zhivotovsky, Damage-induced apoptosis, Oncogene 23 (2004) 2797–2808.
[5] Martin Fussenegger, James E. Bailey, Jeffrey Varner, A mathematical model of caspase function in apoptosis, Nature Biotechnology 18 (2000) 768–774.
[6] Sudhir Gupta, Molecular signaling in death receptor and mitochondrial pathways of apoptosis, International Journal of Oncology 22 (2003) 15–20.
[7] Tin Tin Su, Cellular responses to DNA damage: one signal, multiple choices, Annual Review of Genetics 40 (2006) 187–208.
[8] Vijay Chickarmane, Ali Nadim, Animesh Ray, Herbert M. Sauro, A p53 oscillator model of DNA break repair control, Quantitative Biology-Molecular Networks 1 (2005) arXiv: q- bio. MN/ 0510002 v1.
[9] Jerry E. Chipuk, Lisa Bouchier-Hayes, Tomomi Kuwana, Donald D. Newmeyer, Dougles R. Green, Puma couples the nuclear and cytoplasmic proapoptotic function of p53, Science 309 (2005) 1732–1735.
[10] Lihua Ming, Peng Wang, Alexander Bank, Jian Yu, Lin Zhang, Puma dissociates bax and Bcl-xL to induce apoptosis in colon cancer cells, Journal of Biological Chemistry 281 (2006) 16034–16042.
[11] York Tomita, Natasha Marchenko, Susan Erster, Alice Nemajerova, Alexander Dehner, Christian Klein, Hongguang Pan, Horst Kessler, Petr Pancosta, Ute M. Moll, WT p53 but Not Tumor-derived Mutants, Bind to Bcl2 via the DNA binding domain and induce mitochondrial permeabilization, Journal of Biological Chemistry 281 (2006) 8600–8606.
[12] Narat J. Eungdamrong, Ravi Iyengar, Computational approaches for modeling regulatory cellular networks, Trends in Cell Biology 14 (2004) 661–668.
[13] Réka Albert, Network inference, analysis, and modeling in systems biology, The Plant Cell 19 (2007) 3327–3338.
[14] J.P. Qi, S.H. Shao, Jinli Xie, Y. Zhu, A mathematical model of P53 gene regulatory networks under radiotherapy, Biosystems 90 (2007) 698–706.
[15] Lan Ma, John Wagner, John Jeremy Rice, Wenwei Hu, Arnold J. Levine, Gustavo A. Stolovitzky, a plausible model for the digital response of p53 to DNA damage, PNAS 102 (2005) 14266–14271.
[16] Naama Geva-Zatorsky, Nitzan Rosenfeld, Shalev Itzkovitz, Ron Milo, Alex Sigal, Erez Dekel, Talia Yarnitzky, Yuvalal Liron, Paz Polak, Galit Lahav, Uri Alon, Oscillations and variability in the p53 system, Molecular Systems Biology msb4100068 (2006) E1–E13.
[17] E.Z. Bagci, Y. Vodovotz, T.R. Billiar, G.B. Ermentrout, I. Bahar, Bistability in apoptosis: roles of Bax, Bcl-2, and mitochondrial permeability transition pores, Biophysical Journal 90 (2006) 1546–1559.
[18] Jun Cui, Chun Chen, Haizh Lu, Tingzhe Sun, Pingping Shen, Two independent positive feedbacks and bistability in the Bcl-2 apoptotic switch, Plos One 3 (2008) e1469.
[19] Fei Hua, Melanie G. Cornejo, Michael H. Cardone, Cynthia L. Stokes, Douglas A. Lauffenburger, Effects of Bcl2 Levels on Fas signaling-induced caspase-3 activation: molecular genetic tests of computational model predictions, The Journal of Immunology 175 (2005) 985–995.
[20] Anthony J Raffo, Arianna L Kim, Robert L Fine, Formation of nuclear Bax/p53 complexes is associated with chemotherapy induced apoptosis, Oncogene 19 (2000) 6216–6228.
[21] Harvey Lodish, Arnold Berk, Chris A. Kaiser, Monty Krieger, Matthew P. Scott, Anthony Bretscher, Hidde Ploegh, Paul Matsudaira, Molecular Cell Biology, 6th EditionFreeman, New York, 2008.
[22] Monica Gostissa, Thomas G Hofmann, Hans Will, Giannino Del Sal, Regulation of p53 functions: let's meet at the nuclear bodies, Current Opinion in Cell Biology 15 (2003) 351–357.
[23] Christopher J. Bakkenist, Michael B. Kastan, Initiating cellular stress responses, Cell 118 (2004) 9–17.